

Supporting Information

Shiri and Bird 10.1073/pnas.1700197114

Soot Layer

Substrates are coated with a thin soot layer to create a superhydrophobic surface. To coat the surface, we hold a substrate in a flame so that the soot particles form a spongy black soot layer that makes the surface water repellent (Fig. 1B). The soot deposition thickness can be controlled by varying the deposition time. In our experiments, the average soot thickness is $\sim 28 \pm 2 \mu\text{m}$, as determined through optical microscopy.

Mean Temperature Calculation

The thermographic images provide a surface temperature ($z = 0$) as a function of time t and space. Given the axisymmetry of these results, it is natural to cast the data in cylindrical coordinates around the center of impact. Therefore, the spatially averaged temperature over the footprint area—here approximated by πr_m^2 —is calculated as

$$\bar{T}(z = 0, t) = \frac{1}{\pi r_m^2} \int_0^{2\pi} \int_0^{r_m} T(r, z = 0, t) r dr d\theta. \quad [\text{S1}]$$

Fig. S2 depicts the measured footprint temperature distribution $T(r, z = 0, t)$ for the drop that is illustrated in Fig. 1 of the main text. The surface temperature is warmest in the center and decreases radially. The temperature also decreases with time, denoted by curves with different symbols at different time steps in Fig. S2. The spatially averaged temperature $\bar{T}(z = 0, t)$ that corresponds to this drop is also plotted in Fig. S2.

Because the heat transfer process occurs over a sufficiently short period, we model it as a one-dimensional, semiinfinite body with a pulse boundary condition. With this simplification, the process becomes a function of depth z and time t . Following classic self-similar dynamics, the spatially averaged surface temperature can be written as

$$\bar{T}(z = 0, t) = T_s + \frac{Q}{k_s \pi r_m^2 \sqrt{\pi t / \alpha_s}}. \quad [\text{S2}]$$

Here k_s and α_s are the substrate thermal conductivity and diffusivity, respectively, and Q is the impulse of heat transferred. To calculate Q from experimental data, we use the 60 ms of measurements after the bounce to limit the influence of the longer-time convective heat transfer.

Heat Transfer Mechanism

Heat can be transferred in three different modes: conduction, convection, and radiation. In our analysis, we assume that conduction is the dominant mode. To support this assumption, we compare the rates of heat transfer expected for the parameters corresponding to the experiments. The rate of heat transfer in each mode can be scaled as

$$\dot{Q}_{\text{cond}} = \frac{k_s A \Delta T}{dx} \approx \frac{k_s A \Delta T}{\sqrt{\alpha_s t_r}} \quad [\text{S3a}]$$

$$\dot{Q}_{\text{conv}} = h A \Delta T \quad [\text{S3b}]$$

$$\dot{Q}_{\text{rad}} = \sigma A (T^2 + T_\infty^2) (T + T_\infty) \Delta T. \quad [\text{S3c}]$$

Here T is a substrate temperature, T_∞ is the ambient temperature, h is the convection heat transfer coefficient [which varies between 2 and $25 \left(\frac{\text{W}}{\text{m}^2 \text{K}}\right)$ for free convection of gases], and

$\sigma = 5.67 \times 10^{-8} \left(\frac{\text{W}}{\text{m}^2 \text{K}^4}\right)$ is the Stefan–Boltzmann constant. In our experiments, $k_s = 1.02 - 0.15 \left(\frac{\text{W}}{\text{m}^2 \text{K}}\right)$, $\alpha_s = 4.53 \times 10^{-7} - 0.98 \times 10^{-7} \frac{\text{m}^2}{\text{s}}$, maximum $T = 310 \text{ }^\circ\text{K}$, and $T_\infty = 295 \text{ }^\circ\text{K}$. In addition, t_r varies between 10 ms and 14 ms for drops used in our experiments. To confirm that conduction is the dominant mode, in the following example, we calculate the ratios of heat convection and radiation to conduction for a glass substrate ($k_s = 1.02 \frac{\text{W}}{\text{m}^2 \text{K}}$, $\alpha_s = 4.53 \times 10^{-7} \frac{\text{m}^2}{\text{s}}$) at the maximum temperature $T = 310 \text{ }^\circ\text{K}$ for a residence time of 15 ms, assuming a free convection coefficient $h = 25 \frac{\text{W}}{\text{m}^2 \text{K}}$:

$$\frac{\dot{Q}_{\text{conv}}}{\dot{Q}_{\text{cond}}} \approx \frac{h \sqrt{\alpha_s t_r}}{k_s} \approx 2 \times 10^{-3} \quad [\text{S4a}]$$

$$\frac{\dot{Q}_{\text{rad}}}{\dot{Q}_{\text{cond}}} \approx \frac{\sigma (T^2 + T_\infty^2) (T + T_\infty) \sqrt{\alpha_s t_r}}{k_s} \approx 5 \times 10^{-4}. \quad [\text{S4b}]$$

Because these ratios are much less than unity, convection and radiation effects are negligible relative to conduction, and it is reasonable to neglect them in our analysis.

Material Properties

Table S1 includes material properties used in the calculation of \mathcal{M} .

Hydrophobic and Hydrophilic Feather

The duck feather (Fig. 5A) in our study is naturally superhydrophobic (Fig. S3A) and an impacting water drop bounces off the surface. The same feather can be made superhydrophilic by an air plasma treatment (38) and an impacting water drop will stick and spread along the surface (Fig. S3B). Scanning electron microscopy reveals the barbed hierarchical structure that is typical in veined feathers (Fig. 5B) and responsible for the geometric component of the superhydrophobicity and superhydrophilicity. Before the cold drops impact the surface ($t < 0$), the feather is at ambient conditions, with a temperature $T \approx 24 \text{ }^\circ\text{C}$ (Fig. S3C). Once the drops impact the top, outer surface of the feather, the temperature of the bottom, inner surface begins to cool. For both the superhydrophobic and superhydrophilic conditions, the millimeter water drops are the same temperature $T_b \approx 13 \text{ }^\circ\text{C}$ and fall one after another with the same separation time $dt = 0.6 \text{ s}$. Yet when the drops stick on the surface, the temperature on the bottom of the feather is lowered noticeably more ($\Delta T = 8.45 \text{ }^\circ\text{C}$) than when the drops bounce off the feather ($\Delta T = 2.65 \text{ }^\circ\text{C}$). It is noteworthy that even though the temperature reaches a steady state, the temperature variability around this steady state is larger when the feather is superhydrophobic than when it is superhydrophilic. Closer inspection reveals that this variability is due to a periodic temperature fluctuation with the same period as the separation between the drops dt (Fig. S3C, *Inset*). This temperature periodicity can be interpreted as follows: Each drop removes heat during its 10-ms residence time and the temperature is lowered over a 100-ms timescale from diffusive conduction between the top and the bottom of the feather. Because the feather temperature is below the ambient temperature, it begins to draw in heat from the surroundings and warm up until the process repeats from the impact of the next cold drop.

Experimental Setup for Cooling from Multiple Drops with Heated Feather

The experimental setup used to measure the aggregate cooling of drops dripping on a heated feather is shown in Fig. S4. To

amplify the cooling effect, we also set up the experiment outdoors on a winter day (February 21, 2017) in Boston when the ambient temperature was $T_{atm} = 3.9^\circ\text{C}$. For this setup, a duck feather is clamped at one end and subjected to two streams of water drops from the top. The drops are released from two dispensing needles (16 gauge and 30 gauge) connected to syringes filled with ambient-temperature water. To keep the flow rate of drop streams constant and equal for both drop sizes, a double syringe pump is used. High-speed imaging records the dynamics of the bouncing drops on the top side of the feather. The feather is warmed from underneath to a temperature of $\sim 40^\circ\text{C}$ with a heat gun, to mimic the duck body temperature. A thermal camera measures the temperature along the feather from below.

The experimental data collected from the outdoor experiment are illustrated in Fig. S5. The two streams of water

drops—at an ambient temperature of 3.9°C —bounce on the top side of the feather and locally cool the feather. A heat map in Fig. S5A shows the temperature of the feather from below, averaged over a 6-s period. This temporal average shows that the location opposite to the small dripping drops has a lower average temperature in comparison with the location opposite to the large dripping drops. The temperature within each location of small drops, large drops, and no drops is plotted in Fig. S5B for the 30 s before the drops begin to fall, through the steady dripping, and continuing to a period slightly after the dripping has stopped. An uncontrolled condition outside the laboratory, such as a mild wind, leads to fluctuations in the measured temperature. Despite these large fluctuations, the cooling effect from the bouncing drops is apparent.

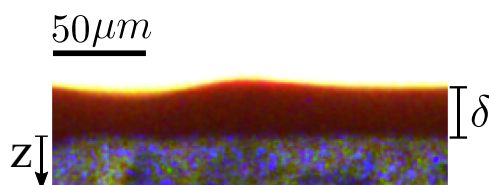


Fig. S1. A composite image illustrating a soot layer coating on a glass slide obtained with an optical microscope. Here the average thickness of the soot layer is $\delta = 28\ \mu\text{m}$ with a root-mean-square roughness of $2\ \mu\text{m}$.

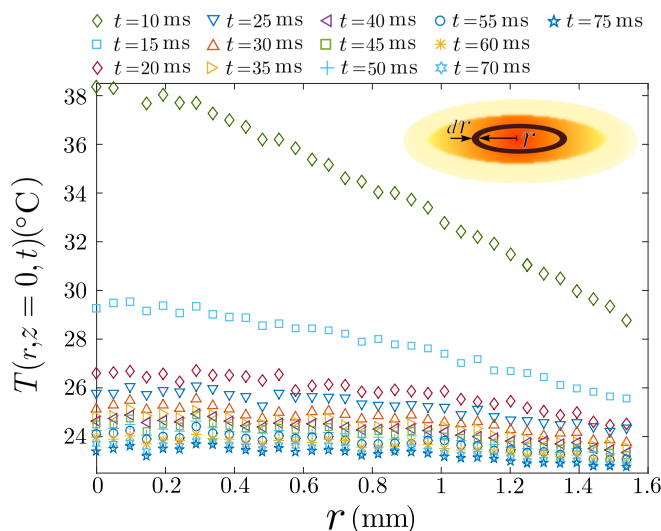


Fig. S2. The footprint temperature as a function of radial position r and time t for the drop illustrated in Fig. 1 of the main text. The spatial average of the temperature $\bar{T}(z=0, t)$ for each time is depicted in Fig. 2 of the main text.

